THIS DOCUMENT PROVIDED BY THE ABBOTT AEROSPACE
TECHNICAL LIBRARY
ABBOTTAEROSPACE.COM

R. & M. No. 2859
(13,066)
A.R.C. Technical Report

MINISTRY OF SUPPLY

AERONAUTICAL RESEARCH COUNCIL
REPORTS AND MEMORANDA

Optical Considerations and Limitations of the Schlieren Method

By

G. S. SPEAK, B.Sc., D.I.C., and D. J. WALTERS, B.Sc., A.Inst.P.

LIBRARY
ROYAL AIRCRAFT ESTABLISHMENT
BEDFORD

Crown Copyright Reserved

LONDON: HER MAJESTY'S STATIONERY OFFICE
1954
SEVEN SHILLINGS NET

This Document Provided by the Abbott Aerospace
TECHNICAL LIBRARY
ABBOTTAEROSPACE.COM

Optical Considerations and Limitations of the Schlieren Method

By

G. S. Speak, B.Sc., D.I.C., and D. J. Walters, B.Sc., A.Inst.P.

Communicated by the Principal Director of Scientific Research (Air), Ministry of Supply

Reports and Memoranda No. 2859*

January, 1950

Summary.—The elementary principles of the schlieren method are first described, with reference to an ideal basic system. Various developments from this basic system are then considered with particular reference to their advantages and disadvantages from the optical point of view. The experimental procedure in setting up the system is also covered from the same aspect.

The general optical theory of the schlieren method is worked out, firstly in terms of the deflection of a ray which passes through a medium of varying refractive index, secondly in terms of the change in illumination caused by this deflection, which is calculated from diffraction theory. Some typical examples are worked out in the latter case.

It is concluded that the schlieren method may be used qualitatively at extremely high sensitivities with satisfactory results, but is not suitable for quantitative work where small pressure or density changes are involved. A secondary conclusion is that the twin-mirror system is in general the best for overall ease of interpretation of results, though local considerations may modify this choice.

1. *Introduction.*—The basic idea of the schlieren or knife-edge method for indicating small optical disturbances was described by Topler some eighty years ago[1], and thirty years later Rayleigh[2] investigated the optical principles involved. In recent years the method has come increasingly into use for the analysis of airflow, and a number of papers, among which may be quoted those of Schardin[3] and Barnes and Bellinger[4]. have been written on the subject from the optical standpoint. The present note is an attempt to fill a need for a treatment which is concerned solely with the practical and theoretical optical limitations of schlieren systems as distinct from descriptions of particular items of equipment of methods of calculating pressure or density distributions in specific cases. Most of the points investigated have been the subject of experiments by the authors and in this way a number of misconceptions and errors by previous workers in this field have been discovered.

2. *Elementary Principles.*—The refractive index (n) of a gas was found by Gladstone and Dale to be related to its density (ρ) by the law

$$k\rho = (n - 1) \quad .. \quad .. \quad .. \quad .. \quad .. \quad .. \quad (1)$$

so that, given the refractive index, the density may be calculated. This property forms the basis of the schlieren and other optical methods of analysing gaseous flow. Light travels at a speed

* R.A.E. Tech. Note I.A.P. 968, received 13th April, 1950.

THIS DOCUMENT PROVIDED BY THE ABBOTT AEROSPACE
TECHNICAL LIBRARY
ABBOTTAEROSPACE.COM

inversely proportional to the refractive index of the medium through which it is passing. Thus, if a light-wave of given form enters a region in which the density varies, it will travel more slowly through zones of high density, and hence high refractive index, than it will through zones of low density. Unless these regions have exactly the same gradient and extent for each part of the wavefront, the latter will thus emerge distorted in shape, and some elements of it will proceed in directions different from those in which they travelled initially. If the change in direction is great enough, the variation in illumination over a screen placed in the light-beam will be different from that which obtained when the density was uniform throughout the path of the beam. This effect is utilised in the shadowgraph method for determining the positions and shapes of shock-waves and other relatively large optical disturbances. As may be supposed however, its use is limited to cases of comparatively steep pressure gradients where the local changes in the direction of travel of the wavefront are large, causing a sharp change in illumination at the corresponding point on the screen.

If the distorted wavefront is compared with the wavefront which would have been obtained had there been no pressure variation in its path, as can be done by means of an interferometer, the changes in refractive index, and hence in pressure or density, which give rise to the distortion can be measured directly by estimation of the displacement of interference fringes at the appropriate points in the disturbed region. The method is simple in principle and sensitive in operation, but adjustments are not easy, and interpretation of the results is somewhat difficult since the nature of the disturbance and the object causing it are masked to some extent by the interference fringes.

The schlieren system overcomes the lack of sensitivity of the shadowgraph method and it gives a picture which is probably easier to interpret qualitatively than that presented by the interferometer. Suppose the original wavefront is so shaped that the light would come to a focus at a small aperture or a narrow slit. If the wavefront is changed in shape by passage through an area of varying refractive index, so that, as before, parts of it change their direction of travel, it is evident that the light from these elements of the wavefront will either miss the aperture completely or will be partially obscured by its edge, depending on the magnitude of the deviations involved and on the size of the aperture. An eye placed behind the aperture and scanning the area of the wavefront would therefore see variations in intensity over the area, depending on the deviations produced at each point, and hence on the density or pressure changes associated with each part of the wavefront. The result may be imagined as a relief map of the wavefront illuminated from one side, so that the general pattern of the pressure changes in a system is quickly comprehended.

The simplest form of schlieren system is illustrated in Fig. 1, where S is a point source of light, imaged as a point at K by the lens L. C is a screen, so placed that an object situated at D would be imaged on it by the lens L, *i.e.*, C and D are conjugate planes. There will be a uniformly illuminated area at C, its size depending on the position of D and the focal length of L. If a knife-edge is moved across the axis of the system at K it will reach a position, if the image at K is truly a point, when it suddenly blocks out all the light proceeding from L to C and the latter darkens uniformly. If now there is a local change of refractive index at the point P in the plane D, the ray SP will be deviated at P. Since it passes through P, which is the conjugate of P′ in the plane C, it must pass through P′ after refraction by the lens, irrespective of its direction through P. It therefore takes the path shown dotted in Fig. 1 and consequently misses the knife-edge, causing a bright patch at P′, the intensity of which may be used to determine the magnitude of the initial deflection, and hence by suitable analysis (*see* section 5.1) the magnitude of the refractive index or density change which produced the deflection.

In practice there would of course be a complete series of deflections, each of which would give rise to a bright patch on the screen, and it would be impossible to discriminate between them. Deflections in the opposite direction to that indicated in the diagram would not show on the screen at all since the knife-edge would stop all light in this direction. The system as described would therefore be impracticable, though its simplicity makes it a useful guide to the principles

This Document Provided by the Abbott Aerospace
TECHNICAL LIBRARY
ABBOTTAEROSPACE.COM

of the method. A more normal system uses a small finite source such as an illuminated slit S (Fig. 2), an image of which is formed at K by the lens L as before. The knife-edge, which is parallel to the slit, is arranged to cut out any desired proportion of the light proceeding through the image to the screen. The light through any point P in the plane D comes from all points in the slit and is focussed by the lens at the point P′ in the screen C. The width of this bundle of rays at K must be the same as that of the image of the slit at K since K and S are conjugate planes, and must therefore be bs/d where s is the slit width and d and b are the distances of the slit and its image from the lens. If the light flux is uniform throughout the beam the proportion of the light through P from S which reaches the screen at P′ must be the ratio of the widths of the partially obscured and unobscured slit images. Thus if this is I/I_0 we have

$$\frac{I}{I_0} = \frac{\left(\frac{bs}{2d} - x\right)}{bs/d} \quad .. \quad .. \quad .. \quad .. \quad .. \quad .. \quad .. \quad (2)$$

where x is the distance which the knife-edge projects beyond the axis.

Suppose now that all the rays which pass through P are deflected at P through a small angle α. They take the paths denoted by dotted lines in Fig. 2 and come to a focus at P′ as before since P′ is the focus of all rays through P which are refracted by L. The base of the cone of rays with apex P′ is moved laterally a distance $a\alpha$ where $a = DL$. From the geometry of the figure it is obvious that the inter-section of this cone by the plane at K remains the same size and shape as before but that it is moved in this plane a distance $(c - b)a\alpha/c$ from its original position, where c is the distance from the lens to the screen. The proportion of the light through P from S which reaches P′ is therefore now given by

$$\frac{I'}{I_0} = \frac{\left(\frac{bs}{2d} - x + a\alpha - \frac{ab\alpha}{c}\right)}{bs/d} \quad .. \quad .. \quad .. \quad .. \quad .. \quad .. \quad (3)$$

Combining (2) and (3). the increment ΔI in intensity at P′ compared with the intensity I before deflection may be written

$$\frac{\Delta I}{I} = \frac{(c - b)}{(bs - 2dx)} \cdot \frac{2ad}{c} \cdot \alpha . \quad .. \quad .. \quad .. \quad .. \quad .. \quad (4)$$

Thus the change in intensity of illumination at P′ can be used to measure the deflection α. This deflection may be either positive or negative so long as it is not so great that the beam either clears the knife-edge completely or is entirely stopped by it.

Examination of equation (4) shows that for high sensitivity of the system the distances d and a of the slit and the disturbed region from the lens should in general be large, while their respective conjugates, the distances b and c of the knife-edge and the screen from the lens should be small. The fairly obvious additional conclusions, that the slit should be small, and that the knife-edge should project as far as possible into the image of the slit, may also be inferred from it. Care should be taken in its interpretation however, particularly when dealing with small deflections. Diffraction, which at all times has some effect, becomes serious in these conditions, and estimates of the limit of sensitivity for examples based on this equation are completely unreliable. This point will be dealt with at a later stage of this note, but is worth mentioning here as some writers have taken this or similar equations for comparison of the relative sensitivities of schlieren, shadowgraph and interferometer systems.

3. *Developments from the Basic System.*—3.1. *Lens Systems.*—The system described above and shown in Fig. 2 has a number of disadvantages. It will be clear that in all cases the size of the disturbance area which can be covered must be less than the lens diameter, and that for reasonably high sensitivity of the system it will not in general exceed one-half of this diameter, since both a and d (Fig. 2) will be large. Consequently if large fields are to be covered the lens may become

This Document Provided by the Abbott Aerospace
Technical Library
abbottaerospace.com

inconveniently large, both in respect of its physical dimensions and of its relative aperture. Since it will have to be corrected for spherical and chromatic aberration to a high degree to prevent deviations being introduced by its own defects, and since in addition these corrections will have to be made for two sets of conjugates, it will be seen that design and manufacture will present some difficulty. Furthermore, inspection of Fig. 2 and equation (4) shows that if high sensitivity is required the image on the screen at C becomes extremely small. One other disadvantage of the system is the fact that the disturbed area must be situated in diverging light, which complicates analysis of the results.

The disturbed area may be placed adjacent to the lens and hence be increased up to the order of size of the latter by using a subsidiary lens behind the knife-edge as in Fig. 3. The subsidiary lens focusses the disturbance region on to the plate, the size of image being controlled by the focal length of this lens and the distance of the disturbed region from it. Consequently the image may be any size consistent with reasonable illumination for viewing or photography, and for a given size of disturbance the main lens will be reduced in aperture compared with the original system. The subsidiary lens does not need to be very highly corrected since it only affects the rays after they focus on the knife-edge, and hence cannot change their deviations; in many cases a spectacle lens will suffice. The main lens of the system must still be highly corrected for both spherical and chromatic aberrations, though now only for one set of conjugates, and the disturbance area will still be situated in diverging light. The system is however much more convenient in application than the first one described and in fact the use of the subsidiary lens for projection of the image is nearly always called for in practice, so much so that its presence will be taken for granted in all the systems which follow.

The disturbance region may be situated in parallel light by using a well-corrected lens with the slit at its focus to produce a collimated beam and then using another similar lens to focus the beam at the knife-edge, as in Fig. 4. The separation of the two lenses may vary within fairly wide limits, thus giving flexibility of positioning of the system, which may be important in practical conditions. The disturbance region may be anywhere along the beam and is focused on the photographic plate or observing screen by means of a subsidiary projection system as above. The displacement produced at the knife-edge depends on the focal length of the second lens and on the deviation at any given point in the disturbed area, but not on the distance of this from the second lens. This may be seen from Fig. 5. where P is any point in the region through which a ray originally passes parallel to the axis and is refracted by the lens L to pass through its principal focus F in the position of the knife-edge, K. If this ray is now deviated through a small angle α, and is looked upon as one of a parallel bundle of rays proceeding at this angle to the lens, L, it is obvious that the complete bundle would come to a focus at F′ where FF′ is $f\alpha$. Consequently the single ray of the bundle which we were considering would pass through this point also, *i.e.* would be displaced laterally $f\alpha$ from its original point of intersection with the plane of the knife-edge. The actual parallelism of the light between the two lenses would obviously be governed by the angular subtense of the slit at the first lens; there is no difficulty in keeping this angle small enough for most purposes, but the effect of irradiating each point in the field by a cone of light of small angle would need to be taken into consideration in the case of very weak deflections.

A double-lens system of the type just described can be made to give satisfactory results if very high sensitivity is not required, and the authors have used two 36-in. f6·3 telephoto lenses with fair success. In all lens systems however, even if the lenses are achromatic, the secondary spectrum is apt to give trouble since it causes coloured fringes in the image of the slit which are cut off by the knife-edge at different rates and so lead to the appearance of coloured patches on the screen. This may be avoided to some extent by using filters or monochromatic light sources, usually however at the expense of greatly reduced intensity of illumination. It will be clear too that the presence of chromatic defects of this nature must tend to reduce the sensitivity of the system since the image of the slit becomes enlarged and blurred as a result.

THIS DOCUMENT PROVIDED BY THE ABBOTT AEROSPACE
TECHNICAL LIBRARY
ABBOTTAEROSPACE.COM

The glass of which the lenses are made must itself be free from refractive index gradients, and inclusions such as air bubbles, or these will appear on the screen and tend to mask the true pattern. The larger the lenses the more difficult and expensive does it become to provide glass of the requisite quality. For this reason, and the fact that chromatic defects can never be completely eliminated in lens systems, mirrors are usually employed instead, particularly if large working-sections are required.

3.2. *Mirror Systems.*—The simplest mirror system consists merely of a concave spherical mirror with the illuminated slit coincident with its centre of curvature, as in Fig. 6. In the absence of any disturbance, rays from the slit S are reflected normally at the mirror M and return towards the centre of curvature. A glass reflector is placed at 34 deg to the mirror axis near the slit to enable the returning rays to fall on the knife-edge K, and thence through the projection system as before. The working-section is placed close up to the mirror to obtain the maximum area. The glass reflector must not of course introduce any deviations itself, but this is relatively easy to ensure in a small component. The system is free from aberrational trouble with the exception of the negligible amount introduced by passage through the reflector. In any event, it is possible to devise arrangements with a single-mirror system which avoid passage of the rays through any refracting medium other than air. The mirror may be of any aperture provided it is spherical within the required limits. An estimate of these limits may be made by reference to Fig. 7 which represents the same arrangement as in Fig. 6 but without the small reflector, the slit and knife-edge being shown coplanar for simplicity. If the slit is width s, then its image will also have this width, and if the knife-edge projects a distance x over the axis the proportion of the original light through the slit which passes the knife-edge will be given by

$$\frac{I}{I_0} = \frac{s/2 - x}{s} \quad \ldots \quad (5)$$

If the rays hitting the point P on the mirror are deflected upwards by a small angle α on reflection because of local imperfections in the mirror surface the image of the slit formed by rays through P will also be displaced upwards through a distance $r\alpha$ where r is the radius of the mirror. Consequently the proportion of the incident light through P which passes the knife-edge is given by

$$\frac{I'}{I_0} = \frac{s/2 - x + r\alpha}{s} \quad \ldots \quad (6)$$

and the fractional increase in illumination $\Delta I/I$ seen in the direction P because of the deformity is thus

$$\frac{\Delta I}{I} = \frac{r\alpha}{s/2 - x} \quad \ldots \quad (7)$$

Now the increase in illumination ΔI which can just be observed by the eye at illumination I varies with I but may be assumed at the order of level of illumination found in these systems to be given by

$$\Delta I/I = 0{\cdot}04 \quad \ldots \quad (8)$$

Taking the radius r to be of the order of 100in. and $(s/2 - x)$ to be of the order of 0·001in. in practical conditions, α may be calculated to be of the order of 4×10^7 radians. Allowing for the reflection, this gives a departure from true sphericity of about 1/25 of a wavelength of light per inch of mirror surface before the change in illumination can be observed by the eye on the screen, that is, before deviations introduced in the working-section begin to be masked by errors in the mirror. It follows that a 10-in. mirror must be spherical within about half a wavelength.

The above argument takes no account of diffraction but is probably reasonably valid for estimating the accuracy of figure required in individual cases. Turning to the disadvantages of the single-mirror system, it will have been noted that, as for the case of the single lens, the light is not parallel, and that it traverses the disturbed region twice. The latter feature tends to make interpretation difficult where large deflections are involved since the same ray may be deflected

THIS DOCUMENT PROVIDED BY THE ABBOTT AEROSPACE
TECHNICAL LIBRARY
ABBOTTAEROSPACE.COM

at two different points in the course of its passage. When the density or pressure gradients are small however the sensitivity may be increased without complications since a ray may pass through practically the same point on both occasions, suffering the same deflection each time and thus being shown up more strongly on the screen than would be the case for single passage.

If the disturbance region is to be situated in parallel light a combination of a concave mirror and a plane mirror may be used as shown in Fig. 8. Here the slit S is off the axis of the concave mirror M, but at its focus, so that a collimated beam is produced on the opposite side of the axis. This is reflected normally at the plane mirror P and returns along its original path as in the previous system. The disturbance region is adjacent to the plane mirror and is traversed twice by the beam. The diagram exaggerates the angle of tilt of the mirror axis. In most cases this tilt will not exceed one or two degrees : it will be clear however that if the disturbance region is to avoid the rays proceeding from and returning to the focus the angle cannot be less than $y/2f$ approximately where $2y$ is the aperture of the mirror and f its focal length. Now by analogy with the result for a single-mirror system, if a is the displacement at the knife-edge of a ray proceeding from a given point on the mirror, the change in illumination ΔI at the appropriate part of the field is given by

$$\frac{\Delta I}{I} = \frac{a}{s/2 - x} \qquad \ldots\ldots\ldots\ldots\ldots\ldots\ldots \quad (9)$$

and normally $(s/2 - x)$ will be made as small as possible to obtain the maximum sensitivity. If the mirror is parabolic in form, the height of the image formed by rays reflected at the centre of the mirror is less than the height of that formed by rays reflected near the margin. That is, the image suffers from coma, and it is readily shown that

$$\frac{\delta h}{h} = \frac{y^2}{4f^2} \qquad \ldots\ldots\ldots\ldots\ldots\ldots\ldots \quad (10)$$

for a single reflection. For two reflections, as in this case, $\delta h/h = y^2/2f^2$ where h, the ideal image height, is given by $h = f \tan \theta$, θ being the angle of tilt of the mirror. We have shown above that θ is never less than $y/2f$ so that a minimum value for δh, the difference in displacement at the knife-edge for rays from the centre and edge of the mirror, is given by

$$\delta h = y^3/4f^2$$

and hence

$$\frac{\Delta I}{I} = \frac{y^3}{4f^2(s/2 - x)} . \qquad \ldots\ldots\ldots\ldots\ldots\ldots\ldots \quad (11)$$

A reasonable value for f would be 100in. and for y (the semi-aperture) would be 5in., which for $(s/2 - x) = 0{\cdot}001$in. (say) leads to

$$\Delta I/I = 3{\cdot}1 .$$

Thus the mirror aberrations lead to uneven illumination of the schlieren field which is easily seen by the eye. It is true that diffraction, which, as will be seen later, can modify the result considerably, has been ignored, and that in practice the slit position can be chosen to give a much improved result. Nevertheless it is obvious that the system is not likely to give high sensitivity, and that matters will be made worse if a spherical mirror, with its higher aberrations, is used rather than a parabolic one. Both mirrors in the system must of course have their figures correct within the order of limits indicated for the previous system, or they will further modify the intensity distribution over the field.

The light passing through the disturbance region can be made parallel, and only traverses the region in one direction, if two concave mirrors are used as in Fig. 9. The light from the slit S falls on the mirror M, at an angle θ to its axis, and is positioned so that the emergent beam, at an angle θ on the other side of the axis, is parallel, This in turn falls on M_2 at an angle to its axis, resulting in an image of the slit at K, where the knife-edge is situated. The disturbance region is placed midway between the two mirrors, free from interference by the light diverging from the slit or converging towards the knife-edge.

THIS DOCUMENT PROVIDED BY THE ABBOTT AEROSPACE
TECHNICAL LIBRARY
ABBOTTAEROSPACE.COM

Now it was pointed out above that a concave mirror used off-axis suffers from coma. This means that in this case the direction of the light reflected from the mirror depends on the position of the point of reflection on the mirror. Referring to Fig. 9, light reflected at O, the centre of the mirror, will proceed to O′, while light reflected at A or B will proceed to A′ or B′, in a slightly different direction, the angle between the two directions being α, where $\alpha = y^2\theta/4f^2$, if θ, the angle of tilt of the mirror, is small. If the second mirror, A′O′B′, is tilted in the direction shown in Fig. 9, it is clear that the ray AB′ will strike it, and proceed towards the slit image at K, in exactly the same sense as the ray BA′ was reflected at the first mirror. Since the angle is very small B′ will, to a close approximation, occupy a similar position on the second mirror to that of B on the first, and the angle of incidence will be the same, so that the aberration (coma) introduced at this reflection will be identical, but of opposite sign, to that introduced at both A and B in the first place. A similar argument holds for the ray BA′; the arrangement is in fact optically symmetrical and the final image at K is free from coma, the aberrations introduced by the reflections at the second mirror annulling those produced at the first.

If the arrangement of mirrors shown in Fig. 10 is used however, the coma is not annulled, but doubled. Taking the ray AB′, B′ now corresponds, from the point of view of symmetry, with the point A on the first mirror. It will occupy the same position on this mirror as A did on the first, to a close approximation but the direction of the normal at B″ is such that the angular error of AB′ compared with OO′ is doubled. The ray BA′ is affected in the same way, leading to an unsymmetrical image at K, which will cause uneven illumination in the field in the same manner as with the single mirror used off-axis which was discussed above. It can be shown in fact that any arrangement of mirrors other than that sketched in Fig. 9 will cause this effect; in particular it should be noted that the two mirror axes should always lie in the same plane.

Although the system shown in Fig. 9 is free from coma, it is not free from astigmatism, and neither is any off-axis mirror system. That is, a point source at S will not be imaged as a point at K, (Fig. 9), but as two line images, at different positions along the line O′K, one in the plane of the paper and perpendicular to O′K, and the other perpendicular to the plane of the paper. If one imagines a slit at S composed of a number of point sources there will thus be a best image position for it where each point is drawn out into a line along the length of the slit, this position along O′K depending on whether the slit is perpendicular to the plane of the paper or in the plane of the paper at right-angles to O′K. If the slit is in any other plane it will clearly be impossible to get an image as narrow and sharp as in these two positions, and one of them should always be chosen. Some applications of the schlieren technique involve observations with the slit (and, of course, the knife-edge) in two directions at right-angles, in order to determine density gradients in these directions. When this is the case the necessary repositioning of the slit and knife-edge should be remembered. An approximate value for the shift of each may be worked out from a knowledge of the positions of the astigmatic foci for a mirror of this nature. Referring to Fig. 11, if M is the mirror, imagined to have parallel light falling on it at an angle θ to its axis, the image perpendicular to the plane of the paper (the tangential image) will be formed at T when $OT = f\cos\theta$, and in the complementary direction the radial or sagittal image will be at S where $OS = f\cos\theta$. These two positions therefore give the best situations for the slit and the knife-edge in the two cases, the distance ST between them being $f\sin^2\theta/\cos\theta$. From Fig. 9 it will be clear that θ will be of the order of $y/2f$ where y is the semi-aperture of a mirror of focal length f. This will usually be small and thus we may write

$$ST = y^2/4f \quad .. \quad .. \quad .. \quad .. \quad .. \quad .. \quad .. \quad .. \quad (12)$$

which for $y = 5$ in. and $f = 100$ in. gives $ST = \frac{1}{16}$ in.

The foregoing relates strictly to parabolic mirrors. If spherical mirrors are used, however, a symmetrical arrangement will remove coma as already described, and the astigmatism will be the same, the only difference being the spherical aberration of the sphere, which is absent in a true paraboloid. Now the equation to a parabola is $y^2 = 4fx$ and to a circle of the same focal

THIS DOCUMENT PROVIDED BY THE ABBOTT AEROSPACE
TECHNICAL LIBRARY
ABBOTTAEROSPACE.COM

length is $y^2 = 4fx - x^2$. It can be shown from this that the abscissa of a point on the parabola only differs from that of a point at the same ordinate y on the circle by an amount δx where

$$\delta x = y^4/64f^3 . \qquad \ldots \ldots \ldots \ldots \ldots \ldots \ldots \quad (13)$$

It follows that a sphere of focal length 100in. and diameter 10in. only departs from the figure of a paraboloid of the same focal length by about half a wavelength of light at the edges, so that for many purposes, particularly where extreme sensitivity is not required, spherical mirrors may be used in the system.

3.3. *Other Devices.*—With any of the systems described above the highest sensitivity is generally obtained when the knife-edge obscures as large a proportion of the slit image as possible. This will be obvious on examining the various equations which have been derived for $\Delta I/I$. It follows that at high sensitivity the illumination in the field is low unless a source of very high brightness is used. Santon[5] has described a system which is reputed to overcome this difficulty, in which a point source is imaged on a small aperture, instead of a knife-edge. The aperture just lets through all the light in the absence of deflections, so that any deflection causes a reduction in intensity at the appropriate point in the image field, the sensitivity primarily depending on the size of aperture employed. Unless a very large proportion of the disturbed region causes deflections there is little doubt that the general level of illumination is higher for the same sensitivity than for the normal method. The sign of the deflection is not determined, however, as it is in the knife-edge system, and since the variety of light sources and photographic plates available make the latter method usable in all except very special cases, the improved illumination given by the Santon method does not usually warrant its use. Fig. 12 shows the general principle of the method.

An ingenious system, due originally to Ronchi, and usable with any of the arrangements described above, substitutes a grid for the knife-edge. The grid is displaced along the axis from the slit image, which is generally arranged to fall in the entrance pupil of the camera or projection lens. The system is shown schematically in Fig. 13. G represents the grid, L_1 the last lens or mirror of the normal schlieren system, L_2 the projection lens, T its focal plane and D the disturbance region. In the absence of deviations, a ray passing through P in the plane of the disturbance region travels parallel to the axis until it is refracted by L_1 at Q towards the slit image S. Without the grid in position it would reach T at the point P′. If one of the opaque lines of the grid stops it, there will be darkness at P′, and at all similar points; it is easily seen that the focal plane T will be traversed by alternate dark and light parallel lines. Now suppose the ray through P is deviated upwards through a small angle θ. It will now be refracted at Q′ on L_1 and after refraction will pass through R in the plane of L_2 where $RS = F\theta$. It is clear that it will not pass through the same point of the grid as it previously did; it still reaches T at the point P′ however, since D and T are conjugate planes, and therefore modifies the illumination at P′, either to light instead of darkness, if it has passed through a clear strip on the grid, or to the darkness corresponding to another opaque grid strip. In either case it will be seen that the original dark line at P′ has been displaced from its original position. Let M be another point in the disturbance plane D, and assume that the ray through M, originally parallel to the axis, has been displaced upwards through a small angle α. After refraction by L_1 at N it travels towards V in the plane of L_2 where $SV = F\alpha$; suppose it is stopped by the grid line which originally stopped the undeviated ray through P. Thus the point M′ in T, the conjugate point to M in D, will be the position to which the original dark band at P′ has been displaced. The displacement P′M′ will be given by PM multiplied by the magnification of the system. From the similar triangles QNA, SAV, since

$$VS = F\alpha , \qquad QN = \frac{F(F-l)}{l}\,\alpha ,$$

whence

$$PM = QN + d\alpha = \alpha\left[\frac{F^2}{l} + d - F\right].$$

THIS DOCUMENT PROVIDED BY THE ABBOTT AEROSPACE
TECHNICAL LIBRARY
ABBOTTAEROSPACE.COM

If b is the distance from the second principal point of the projection lens to its focal plane, the magnification of the system is given by

$$\frac{F}{d-F} \cdot \frac{b(d-F)}{F^2} = \frac{b}{F}.$$

Thus the fringe shift $P'M'$ becomes

$$P'M' = \frac{b}{F} PM = \alpha \left[\frac{Fb}{l} + \frac{b(d-F)}{F} \right] \quad .. \quad .. \quad .. \quad .. \quad (14)$$

$$= K\alpha \quad .. \quad .. \quad .. \quad .. \quad .. \quad .. \quad .. \quad .. \quad (15)$$

where K is a constant for a given system, and is independent of the characteristics of the grid. The fringe shift thus measures the deviation at the point in the field corresponding to the displaced part of the fringe. It is obviously an advantage to have as many fringes crossing the field as possible. The grid however acts as a diffraction grating and diffraction fringes occur around the images on T and affect the definition and sensitivity of the system. If the working distance of the camera lens is b as before, the spaces in the grid are of width x and the wavelength of the light used is λ, the separation of the successive diffraction fringes from each other is given by

$$s = \lambda b/x \quad .. \quad .. \quad .. \quad .. \quad .. \quad .. \quad .. \quad .. \quad (16)$$

These of course diminish rapidly in intensity as their distance from the main image increases but enough may be seen to affect definition seriously. For example if d is 15 in., $\lambda = 0{\cdot}000022$ in. and $x = 0{\cdot}01$ in. (50 lines/in.), s is $0{\cdot}033$ in. and the diffraction maxima are easily visible. Reducing the number of lines per inch and increasing l, the distance of the grid from the slit image, in proportion, will reduce the diffraction effect while keeping the total number of grid fringes in the image the same, but reference to equation (14) will show that the sensitivity is impaired since high sensitivity is given by a small l. A compromise has thus to be effected which gives reasonably high potential sensitivity together with a standard of definition which enables this sensitivity to be utilised. It should be noted that varying the ratio of the widths of opaque and clear strips on the grid modifies the diffraction effect and may help in some cases to improve matters. A sensitivity sufficiently high to enable deflections of the order of a few seconds to be measured can be attained, but the system is more often used to measure relatively high deflections. A special case of the Ronchi method is worth mentioning here. If the grid is arranged to lie in the position normally occupied by the knife-edge, *i.e.*, in the plane of the slit image, and the spacing of the bars is such that this image is no wider than one clear aperture of the grid, there will be uniform intensity on the screen at T (Fig. 14) in the absence of any disturbance in the beam. If any deflections occur the affected rays will strike other parts of the grid and will pass through another aperture or be stopped by a bar depending on the magnitude of the displacement. A contour pattern should result on the screen, consisting of lines of equal displacement or isophots as Schardin has called them. In theory this should be a very useful application of the schlieren method, in practice, however, the grid lines have to be so close together, if successive contour lines are to represent reasonably small increments in deviation angle, that the diffraction effect mentioned above comes into play and the resulting diffraction fringes in the image confuse matters seriously.

4. *Experimental Procedure.*—In the great majority of cases the source of light in any schlieren system is a slit, which is imaged by the mirrors or lenses into the plane of the knife-edge and parallel to it.

A condensing system, preferably achromatic unless monochromatic light is to be used, projects the image of the original light source on to the slit. In order to obtain exact parallelism of the slit image and the knife-edge, and so achieve the maximum sensitivity, particularly when astigmatism is present, as in most of the mirror systems described above, some care is needed in the initial adjustments. The writers observe the image of the slit (suitably reduced in

This Document Provided by the Abbott Aerospace
TECHNICAL LIBRARY
ABBOTTAEROSPACE.COM

intensity), and the knife-edge, with a low-powered microscope so that they are easily set parallel. If astigmatism is present a small pinhole is placed over the original slit and the direction of the astigmatic line image of this pinhole is noted. The pinhole is then removed and the slit rotated until it lies in the same direction as this image, the knife-edge finally being adjusted until it is parallel to it. Taylor and Waldram[5] use two lenses behind the knife-edge, one of which is removable. When one only is used (L_1 in Fig. 15), a magnified image of the slit image is formed on the screen. When the second lens L_2 is added the disturbance region is automatically focussed on the screen. It is then possible easily and quickly to tell whether the system is at any time being used in a condition of high sensitivity, *i.e.*, with slit image and knife-edge parallel.

The knife-edge is placed in the same position as the slit image by observation of the manner in which the field darkens as the knife-edge is moved across the image, the ideal of course being uniform darkening. If the field darkens from one side, in the same direction as the knife-edge moves, then the slit image is falling short of the knife-edge. If the shadow moves across the field in the opposite direction, the reverse is true; Fig. 16 shows schematically the reason for this.

It is possible to use any shape of source instead of a slit provided that the knife-edge is complementary in shape in order to obtain uniform sensitivity over its extent. To ensure this a photographic plate may be exposed in the image position for a source of any shape and replaced after development so as to act as the knife-edge. It will be clear that only light which is deflected within the system will pass the 'knife-edge', with the exception of that which is diffracted round its boundaries. With a source which is irregular in shape, however, deflections in several directions will record on the screen and hence interpretation of the results becomes a matter of some difficulty. The presence of astigmatism in the system will also further complicate matters if such a source is employed as the astigmatic foci of the different parts of the source lie at different points. Unless a very elementary analysis is sufficient, therefore, it is unwise to use this method.

When used in the normal manner, with a slit source and a knife-edge, the deflections which are recorded are those perpendicular to the knife-edge direction or the components in this direction. By taking a photograph with the knife-edge and slit pointing in one direction and then a second one with the two turned through a right-angle the direction and magnitude of all deflections can be determined since their components in two directions at right-angles can be calculated. It has been suggested that the same effect can be obtained with a single exposure if two slits at right-angles and two corresponding knife-edges are used. It can be shown however that a knife-edge of this type, *i.e.*, L-shaped, gives an effect which is simply equivalent to that obtained with a single straight knife-edge and slit pointing in the direction given by joining the two ends of the L. Thus consider Fig. 17 which shows the L-shaped system with arms of length l_1 and l_2 and the equivalent straight-edge of length $\sqrt{(l_1^2 + l_2^2)}$. Suppose the image of the slit (L-shaped and straight in turn) is deflected through a small distance in any direction, the components of the shift perpendicular to the two arms of the L being a_1 and a_2 respectively. These deflections are assumed to be less than the slit width in each case and to be small compared with the length of slit. Then the change in illumination at the appropriate point on the screen is proportional to $(l_1a_1 + l_2a_2)$. The full deflection is $\sqrt{(a_1^2 + a_2^2)}$ in a direction given by direction cosines $a_1/\sqrt{(a_1^2 + a_2^2)}$ and $a^2/\sqrt{(a_1^2 + a_2^2)}$. The direction cosines of the perpendicular to the straight-edge are $l_1/\sqrt{(l_1^2 + l_2^2)}$ and $l_2/\sqrt{(l_1^2 + l_2^2)}$. It follows therefore that the component of the deflection in this latter direction is $(l_1a_1 + l_2a_2)/\sqrt{(l_1^2 + l_2^2)}$ and that since the change in illumination is proportion to the deflection component multiplied by the slit length, this must be $(l_1a_1 + l_2a_2)$ as for the L-shaped system. The ratio of the change in illumination to the original illumination $(\Delta I/I)$ is of course independent of the length of the straight-edge, so that the two systems must produce exactly the same effect at the screen so long as the straight-edge points in the right direction, irrespective of its length. A similar argument holds when the source and its image are circular and cut by an L-shaped edge, the system giving an effect which could be produced by a single knife-edge.

THIS DOCUMENT PROVIDED BY THE ABBOTT AEROSPACE
TECHNICAL LIBRARY
ABBOTTAEROSPACE.COM

5. *The General Theory of the Schlieren Method.*—5.1. *The Relationship between Deflection and Density or Refractive Index Variations in the Disturbance Region.*—Suppose a co-ordinate system $O\,xyz$, the z-direction being the axis of the schlieren system in the disturbance region, andl et the refractive index at any point be defined by $\mu(xyz) = K$. Take an incident ray parallel to the z-axis entering this region; its direction cosines will be 0, 0, 1, and after passing through a small element of the system may be taken as $\delta\alpha$, $\delta\beta$, 1, assuming that both $\delta\alpha$ and $\delta\beta$ are small. If the point of incidence of the ray is (x, y, z) the normal to the surface $\mu(x, y, z) = K$ at this point has direction cosines given by co-ordinate geometry as proportional to $\partial\mu/\partial x$, $\partial\mu/\partial y$, $\partial\mu/\partial z$; suppose their actual values are $n\partial\mu/\partial x$, $n\partial\mu/\partial y$, $n\partial\mu/\partial z$ where n is a constant. By the laws of refraction this normal must be co-planar with the incident and refracted rays and the condition for this is

$$\begin{vmatrix} 0 & 0 & 1 \\ \delta\alpha & \delta\beta & 1 \\ n\dfrac{\partial\mu}{\partial x} & n\dfrac{\partial\mu}{\partial y} & n\dfrac{\partial\mu}{\partial z} \end{vmatrix} = 0 . \qquad \ldots\ldots\ldots\ldots\ldots \quad (17)$$

Expanding this determinant leads to the equation

$$\delta\alpha \,.\, \frac{\partial\mu}{\partial y} = \delta\beta \,.\, \frac{\partial\mu}{\partial x} . \qquad \ldots\ldots\ldots\ldots\ldots\ldots \quad (18)$$

If θ is the angle included between the incident ray and the normal, and θ' that between the refracted ray and the normal, and the refractive index changes from μ to $\mu + \delta\mu$ across the small element which we are considering, we have firstly, from the values for the direction cosines

$$\cos\theta = n\frac{\partial\mu}{\partial z} \qquad \ldots\ldots\ldots\ldots\ldots\ldots \quad (19)$$

and

$$\cos\theta' = n\,\delta\alpha \,.\, \frac{\partial\mu}{\partial x} + n\,\delta\beta \,.\, \frac{\partial\mu}{\partial y} + n\frac{\partial\mu}{\partial z} \qquad \ldots\ldots\ldots\ldots \quad (20)$$

and secondly, by Snell's law

$$\mu \sin\theta = (\mu + \delta\mu)\sin\theta' . \qquad \ldots\ldots\ldots\ldots\ldots \quad (21)$$

Squaring equation (21) and neglecting powers of $\delta\mu$ higher than the first leads to

$$(1 - \cos^2\theta)\left(1 - 2\frac{\lambda\mu}{\mu}\right) = 1 - \cos^2\theta'$$

whence

$$\cos^2\theta' = \cos^2\theta\left(1 + 2\frac{\delta\mu}{\mu}\tan^2\theta\right) \qquad \ldots\ldots\ldots\ldots \quad (22)$$

or

$$\cos\theta' = \cos\theta\left(1 + \frac{\partial\mu}{\mu}\tan^2\theta\right).$$

Substituting in (22) for $\cos\theta'$ and $\cos\theta$ from (19) and (20) we get

$$n\,\delta\alpha = \frac{\partial\mu}{\partial z} + n\delta\beta \,.\, \frac{\partial\mu}{\partial y} + n\frac{\partial\mu}{\partial z} = n\frac{\partial\mu}{\partial z}\left[1 + \frac{\partial\mu}{\mu}\left\{1 - n^2\left(\frac{\partial\mu}{\partial z}\right)^2\right\}\Big/ n^2\left(\frac{\partial\mu}{\partial z}\right)^2\right].$$

Substituting for $\delta\beta$ from (18) and dividing throughout by n leads to

$$\delta\alpha\left[\frac{\partial\mu}{\partial x} + \left(\frac{\partial\mu}{\partial y}\right)^2\Big/\frac{\partial\mu}{\partial x}\right] = \frac{\partial\mu}{\mu}\left[1 - \left(n\frac{\partial\mu}{\partial z}\right)^2\right]\Big/ n^2\frac{\partial\mu}{\partial z} . \qquad \ldots\ldots\ldots \quad (23)$$

THIS DOCUMENT PROVIDED BY THE ABBOTT AEROSPACE
TECHNICAL LIBRARY
ABBOTTAEROSPACE.COM

Since

$$n^2\left[\left(\frac{\partial\mu}{\partial x}\right)^2+\left(\frac{\partial\mu}{\partial y}\right)^2+\left(\frac{\partial\mu}{\partial z}\right)^2\right]=1$$

the left-hand side of Equation (23) becomes

$$\delta\alpha\left[\frac{1-\left(n\frac{\partial\mu}{\partial z}\right)^2}{n^2}\right]\Big/\frac{\partial\mu}{\partial x}$$

and thus the complete equation may be re-written as

$$\delta\alpha\Big/\frac{\partial\mu}{\partial x}=\frac{\partial\mu}{\mu}\Big/\frac{\partial\mu}{\partial z}$$

or

$$\delta\alpha=\frac{1}{\mu}\frac{\partial\mu}{\partial x}\,\delta z$$

and hence

$$\delta\beta=\frac{1}{\mu}\frac{\partial\mu}{\partial y}\,\delta z \qquad \text{from (18)}$$

. . . . . (24)

Since the direction cosine in the z-direction remains unity, $\delta\alpha$ and $\delta\beta$, being small, are the components along the x and y axes respectively of the increment in deflection of the ray. Thus the components of the final deflection after passage through the disturbed region, assuming, as is implicit in the use of the schlieren method, that this is not large, are given by

$$\alpha=\int_{z0}^{z1}\frac{1}{\mu}\frac{\partial\mu}{\partial x}\,dz \qquad \text{. . . . . (25)}$$

and

$$\beta=\int_{z0}^{z1}\frac{1}{\mu}\frac{\partial\mu}{\partial y}\,dz$$

where z_0 and z_1, represent the z-co-ordinates of the start and finish of the disturbance region.

If now the refractive index μ is given as a function of position the resulting deflection can be calculated. Actually of course the reverse is usually the case ; the deflection is measured in the schlieren system and the refractive index distribution is required. This usually involves the assumption of a general type of distribution. For example, if a cylindrical field around the z-axis is assumed, so that μ, $\partial\mu/\partial x$ and $\partial\mu/\partial y$ are independent of z, we get

$$\frac{\partial\mu}{\partial x}=\frac{\mu\alpha}{z_1-z_0}$$

and

$$\frac{\partial\mu}{\partial y}=\frac{\mu\beta}{z_1-z_0}$$

. . . . . (26)

The model being examined in the wind tunnel is usually enclosed between two plane-parallel glass plates, which introduce no deflection themselves. The air outside them has a constant refractive index μ_0 and if the deflections as measured in this region are denoted by α' and β' we have by Snell's law

$$\mu\alpha=\mu_0\alpha'$$
$$\mu\beta=\mu_0\beta'$$

. . . . . (27)

THIS DOCUMENT PROVIDED BY THE ABBOTT AEROSPACE
TECHNICAL LIBRARY
ABBOTTAEROSPACE.COM

Substituting in equation (26) leads to the conditions

$$\frac{\partial \mu}{\partial x} = \frac{\mu_0 \alpha'}{z_1 - z_0}$$

$$\frac{\partial \mu}{\partial y} = \frac{\mu_0 \beta'}{z_1 - z_0} \qquad \ldots \ldots \ldots \ldots \ldots \ldots \ldots \quad (28)$$

or $\partial\mu/\partial x = k\alpha'$ and $\partial\mu/\partial y = k\beta'$, where k is a constant for a given set of conditions; thus the refractive index gradients are easily determined, and hence the pressure or density gradients, *via* equation (1). Schardin deals with the cases of a rotationally symmetrical field and a field with spherical symmetry in addition to the cylindrical field, and other special cases could be worked out. We are concerned here, however, with the general optical principles of the method and therefore confine ourselves to noting that the simple equations (24) and (25), and consequent simplicity of equation (28) and similar equations with other types of field, arise from the fact that the incident ray has been assumed parallel to the axis. In other words the use of the two-mirror or two-lens system with parallel light irradiating the striation region would be necessary for these equations to be valid. If the light passing through this region is not parallel the evaluation of the results is much more difficult. Assuming direction cosines a, b, c, for the incident ray it may be shown by similar reasoning to that given above that the components $\delta\alpha$, $\delta\beta$ of the increment in deflection parallel to x and y axes respectively are given by

$$\left.\begin{aligned} \delta\alpha &= \frac{\delta\mu}{\mu} \cdot \frac{\left[c\frac{\partial\mu}{\partial x} - a\frac{\partial\mu}{\partial z}\right]}{\left[a\frac{\partial\mu}{\partial x} + b\frac{\partial\mu}{\partial y} + c\frac{\partial\mu}{\partial z}\right]} \\ \text{and} \quad \delta\beta &= \frac{\delta\mu}{\mu} \cdot \frac{\left[c\frac{\partial\mu}{\partial y} - b\frac{\partial\mu}{\partial z}\right]}{\left[a\frac{\partial\mu}{\partial x} + b\frac{\partial\mu}{\partial y} + c\frac{\partial\mu}{\partial z}\right]} \end{aligned}\right\} \qquad \ldots \ldots \ldots \ldots \quad (29)$$

which reduce to (24) when $a = b = 0$ and $c = 1$. Even assuming a cylindrical refractive index distribution, $\left(\frac{\partial\mu}{\partial z} = 0\right)$, the integration of these two quantities to get the full deflections α and β presents some difficulty. It is clear therefore that the use of a parallel beam is essential if quantitative results are required with a minimum of analysis of the schlieren pattern.

The relationship between the deflection of a ray and the refractive index distribution in the medium through which it passes, which has been derived above, is completely valid, whether looked at from the point of view of geometric or physical optics theory. The connection between the deflection and the intensity change at the final focal plane, however, depends on the method of approach. The geometric theory was used in section 2 above to show that the deflection of a ray is proportional to the fractional intensity change at the corresponding field point. It will be shown later that the more accurate physical or wave theory of optics leads to the conclusion that this relationship is only correct for relatively large deflections and low sensitivity of the system; consequently it is not always possible to apply equations (25) *et seq* in practice.

5.2. *The Intensity Distribution in the Schlieren Field.*—The simple treatment of the theory of the schlieren system, leading to expressions for the change of intensity arising from a given deflection at a point in the field, was based on geometrical optics and took no account of diffraction or wave theory. It is important that the latter should not be overlooked, as not only can it explain effects which it is impossible to demonstrate by the methods of geometrical optics, but its neglect in some circumstances leads to completely erroneous results. It will be assumed in the discussion which follows, which is based on the wave theory of light, that the source of

THIS DOCUMENT PROVIDED BY THE ABBOTT AEROSPACE
TECHNICAL LIBRARY
ABBOTTAEROSPACE.COM

light is an infinitely narrow slit situated at the focus of a lens (or mirror) which is followed by a second lens or mirror to bring the parallel rays between the two to a focus. Further assumptions are that all apertures in the system are rectangular and that all the elementary sources distributed uniformly along the length of the slit are in one phase, so that the problem may be considered in two dimensions, and, lastly, that the effect of a screen in the system is merely to stop those parts of the wave which impinge upon it, without influencing the neighbouring parts. The two last assumptions cannot be strictly true but are sufficiently near the truth not to affect any results very seriously, and the assumption of rectangular apertures probably approximates more closely to conditions in a wind tunnel than would circular ones. The basic method of approach is due originally to Lord Rayleigh (*loc. cit.*); in recent years Linfoot[6] and others have adopted a more rigorous, three-dimensional treatment, which however, need not be reproduced here.

In Fig. 18, let A be the second lens of the system, bringing the parallel rays, which emerge from the first lens, to a focus at B. At B are two adjustable screens or knife-edges, parallel to one of the sides of the rectangular aperture of the system and to the slit and its image. Immediately behind B is the camera lens or observer's eye L. Diffraction will cause the image of the original infinitely narrow slit to be spread out at B with a fairly narrow maximum and several secondary maxima (diffraction bands) extending to infinity on each side. Each point in the second aperture at B will be irradiated with light over a finite angle and the intensity looking in a direction making an angle ϕ with the axis will be compounded of all the disturbances in the direction ϕ through all such points Q over the aperture. This is strictly true only if the lens L is focussed for infinity *i.e.*, so as to receive parallel bundles of rays, but in practice this will be very nearly the case. P is a point in the first aperture, AP $= y$, BQ $= x$, AB $= f$. If V is the velocity of propagation of the wave, the disturbance at a point distance d from the origin may be represented by $\sin (2\pi/\lambda)(Vt - d)$ where λ is the wavelength and t the time. The distance from P to Q is less than PB by an amount yx/f, and since PB $= f$ to a good enough approximation the vibration at Q arising from all points P in the first aperture is given by

$$\int \sin \frac{2\pi}{\lambda}\left(Vt - f + \frac{xy}{f}\right) dy$$

or, if

$$\frac{2\pi}{\lambda} = k \text{ and } \frac{y}{f} = \theta ,$$

by

$$\int_{-\theta}^{\theta} \sin k(Vt - f + x\theta)\, d\theta \qquad .. \quad .. \quad .. \quad .. \quad .. \quad (30)$$

the limits of integration corresponding to the angular aperture of lens A. Writing $T = (Vt - f)$ and expanding, (30) becomes

$$\sin kT \int_{-\theta}^{\theta} \cos kx\theta\, d\theta + \cos kT \int_{-\theta}^{\theta} \sin k\theta\, d\theta$$

or simply

$$2 \sin kT \frac{\sin kx\theta}{kx} \qquad .. \quad .. \quad .. \quad .. \quad .. \quad .. \quad (31)$$

which, ignoring the constant term $\sin kT$, and squaring, gives the intensity in the image of the slit at any height x in the plane BQ.

If we now consider what is to be observed in the direction ϕ through the second aperture it should be noted that if a line is drawn through the axis perpendicular to the parallel bundle of inclination ϕ, such a line represents the wavefront travelling eventually to a point in the focal plane of lens L. A vibration starting at height x in the plane BQ will be retarded an amount $x\phi$ approximately relative to one starting on the axis. It will also have an initial amplitude $2 \sin kx\theta/kx$, so that the complete vibration from this point is given by

$$2 \sin k(T + \phi x) \frac{\sin kx\theta}{kx} .$$

THIS DOCUMENT PROVIDED BY THE ABBOTT AEROSPACE
TECHNICAL LIBRARY
ABBOTTAEROSPACE.COM

To determine the full effect of all the vibrations over the second aperture we have to integrate over this aperture, giving

$$2\int \sin k(T+\phi x)\,\frac{\sin kx\theta}{kx}\,dx$$

or

$$\sin kT\int\frac{[\sin k(\theta+\phi)x+\sin k(\theta-\phi)x]}{kx}\,dx+\cos kT\int\frac{[\cos k(\theta-\phi)x-\cos k(\theta+\phi)x]}{kx}\,dx\,. \qquad (32)$$

The intensity of the disturbance is given by the sum of the squares of the coefficients of $\sin kT$ and $\cos kT$, i.e., by the sum of the squares of the integrals. If we note the definitions of the sine and cosine integrals,

$$\text{Si}\,(x)\ \text{ and }\ \text{Ci}\,(x)$$

as

$$\text{Si}\,(x)=\int_0^x\frac{\sin x}{x}\,dx\ \text{ and }\ \text{Ci}\,(x)=\int_\infty^x\frac{\cos x}{x}\,dx$$

and take the limits of x as x_1 and x_2, (32) becomes

$$\sin kT\Big[\text{Si}\,k(\theta+\phi)x+\text{Si}\,k(\theta-\phi)x\Big]_{x_1}^{x_2}+\cos kT\Big[\text{Ci}\,k(\theta-\phi)x-\text{Ci}\,k(\theta+\phi)x\Big]_{x_1}^{x_2}. \qquad (33)$$

The limits x_1 and x_2 of the second aperture may be chosen to be of any value. In particular, if x_2 is large, limited only by the aperture of the camera lens, and x_1 is small, the effect of the knife-edge in the schlieren system is obtained, and (33) may be used to calculate the intensity distribution over the field in the absence of any deflections. In a practical case the semi-aperture of the lens or mirror A is likely to be of the order of 5 in. and its focal length f say 120 in. (40π in approximately). The wavelength λ will be say 1/40,000 in. and x_2, the semi-aperture of the camera lens, about $\frac{1}{2}$ in. Thus $k\theta x_2=2\pi\theta x_2/\lambda=5{,}000$. If the knife-edge is situated exactly on the axis of the system $x_1=0$. In this case the coefficient of $\sin kT$ in (33) becomes

$$\text{Si}\left[5000\left(1+\frac{\phi}{\theta}\right)\right]+\text{Si}\left[5000\left(1-\frac{\phi}{\theta}\right)\right] \qquad .. \quad .. \quad .. \quad (34)$$

and by expressing Ci (x) as an infinite series* in ascending powers of x, the coefficient of $\cos kT$ may be shown to be

$$\text{Ci}\left[5000\left(1-\frac{\phi}{\theta}\right)\right]-\text{Ci}\left[5000\left(1+\frac{\phi}{\theta}\right)\right]+\log_e\left(1+\frac{\phi}{\theta}\right)-\log_e\left(1-\frac{\phi}{\theta}\right) \quad .. \quad (35)$$

---

* These series are as follows, for moderate values of x —

$$\text{Si}\,(x)=x-\frac{1}{3}\cdot\frac{x^3}{3!}+\frac{1}{5}\cdot\frac{x^5}{5!}-\ldots$$

and

$$\text{Ci}\,(x)=\gamma+\frac{1}{2}\log_e(x^2)-\frac{1}{2}\cdot\frac{x^2}{2!}+\frac{1}{4}\cdot\frac{x^4}{4!}-\ldots$$

where $\gamma=$ Euler's constant $=0{\cdot}5772157$.

For large values of x the following series may be used

$$\text{Si}\,(x)=\frac{\pi}{2}-\cos x\left\{\frac{1}{x}-\frac{2!}{x^3}+\frac{4!}{x^5}-\ldots.\right\}-\sin x\left\{\frac{1}{x^2}-\frac{3!}{x^4}+\frac{5!}{x^6}-\ldots\right\}$$

and

$$\text{Ci}\,(x)=\sin x\left\{\frac{1}{x}\frac{2!}{x^3}+\frac{4!}{x^5}-\ldots..\right\}-\cos x\left\{\frac{1}{x^2}-\frac{3!}{x^4}+\frac{5!}{x^6}-\ldots..\right\}.$$

THIS DOCUMENT PROVIDED BY THE ABBOTT AEROSPACE
TECHNICAL LIBRARY
ABBOTTAEROSPACE.COM

so that the intensity of illumination at the proportion of the full field given by ϕ/θ may be calculated. At the edge of the field, where $\phi/\theta = 1$ it should be noted that (35) becomes

$$\gamma + \log_e(10000) \quad .. \quad .. \quad .. \quad .. \quad .. \quad .. \quad (36)$$

by again applying the infinite series to avoid indeterminate quantities. Squaring (34) and (35) and adding for each value of ϕ/θ, gives the curve of illumination over the field, which is obviously symmetrical about the axis. The individual values are listed in Table 1 and plotted in Fig. 19 as the logarithm of illumination against field position. This is done because a logarithmic plot gives a much better sense of what the eye would appreciate when looking at the field or at a photographic plate exposed in the system. It will be seen that illumination is fairly uniform over a large part of the field but suddenly increases at the edge and is fairly appreciable for some way outside the actual physical boundary of the aperture. This bright edge is in fact noticeable in all schlieren systems and is also seen around any obstacles in the field, as might be expected since they are in effect part of the limiting aperture. It should be noted that, whereas geometrical optics would lead one to expect a uniformly illuminated field, the intensity actually varies over a range of 10 : 1.

In practice the general field would be darkened much more than has been supposed above where only half the light reaching the knife-edge has been cut off. It was mentioned above that the light distribution in the knife-edge plane consists of a bright axial band with other less bright fringes extending to infinity on each side. The intensity at any distance x from the axis is given by (31) as proportional to $\sin^2 kx\theta/k^2x^2$, being zero at the points given by $kx\theta = n\pi$, where $n = 1, 2, 3$, etc. The total light in the diffraction pattern between the axis and the point x is therefore given by

$$J_x = \int_0^x \frac{\sin^2 k\theta x}{k^2x^2}\, dx$$

and the proportion of this to the whole of the light in the complete distribution is

$$\frac{J_x}{J_\infty} = \int_0^x \frac{\sin^2 k\theta x}{k^2x^2}\, dx \Big/ \int_0^\infty \frac{\sin^2 k\theta x}{k^2x^2}\, dx \quad .. \quad .. \quad .. \quad .. \quad (37)$$

which on integration gives

$$\frac{J_x}{J_\infty} = \frac{2}{\pi}\left[\mathrm{Si}\,(2k\theta x) - \frac{\sin^2 k\theta x}{k\theta x}\right]. \quad .. \quad .. \quad .. \quad .. \quad (38)$$

The edge of the central bright fringe is obtained where $k\theta x = \pi$; putting this in (38) gives

$$\frac{J_x}{J_\infty} = 0{\cdot}903\,,$$

so that nine-tenths of the total light goes into this band. A reasonable setting of the knife-edge in a practical system would correspond to this position for x, the knife-edge actually cutting off all the light on one side of the axis and up to the edge of the central band on the other side, thus resulting in about 5 per cent of the original light being transmitted. Equation (23) would then become, with $k\theta x_1 = \pi$ and $k\theta x_2 = 5{,}000$ as before :

$$\sin kT\left[\mathrm{Si}\left\{5000\left(1+\frac{\phi}{\theta}\right)\right\} + \mathrm{Si}\left\{5000\left(1-\frac{\phi}{\theta}\right)\right\} - \mathrm{Si}\,\pi\left(1+\frac{\phi}{\theta}\right) - \mathrm{Si}\,\pi\left(1-\frac{\phi}{\theta}\right)\right]$$

$$+ \cos kT\left[\mathrm{Ci}\left\{5000\left(1-\frac{\phi}{\theta}\right)\right\} - \mathrm{Ci}\left\{5000\left(1+\frac{\phi}{\theta}\right)\right\} + \mathrm{Ci}\,\pi\left(1+\frac{\phi}{\theta}\right) - \mathrm{Ci}\,\pi\left(1-\frac{\phi}{\theta}\right)\right]. \quad (39)$$

Table 2 gives the values of intensity across the field for this setting and Fig. 19 shows the plot of log I against field position as before. It will be seen that the intensity, while symmetrical about the axis, changes at a greater rate than was the case with the previous knife-edge position, being doubled at about two-thirds of the maximum field diameter. The bright edge is also more marked compared with the axial intensity.

THIS DOCUMENT PROVIDED BY THE ABBOTT AEROSPACE
TECHNICAL LIBRARY
ABBOTTAEROSPACE.COM

If the knife-edge is removed completely, leaving the (rectangular) boundary of the camera lens as the limiting aperture, so that in (33) $x_2 = x = -x_1$, the coefficient of cos kT vanishes and the intensity becomes simply

$$4[\text{Si } k(\theta + \phi)x + \text{Si } k(\theta - \phi)x]^2 \quad \ldots \quad \ldots \quad \ldots \quad \ldots \quad (40)$$

or, in putting $k\theta x = 5{,}000$ to correspond with the two cases just mentioned,

$$4\left[\text{Si}\left\{5000\left(1 + \frac{\phi}{\theta}\right)\right\} + \text{Si}\left\{5000\left(1 - \frac{\phi}{\theta}\right)\right\}\right]^2.$$

These values are listed in Table 3 and plotted in Fig. 19. The bright edge has, to all intents and purposes, disappeared, and the field has uniform intensity with a sharp transition to zero intensity at the edge of the field. It will be clear from a study of the curves in Fig. 19 that the effect of moving in the knife-edge is a symmetrical darkening of the field, which however becomes less uniform in intensity as more light is cut off. Geometric optics would lead one to suppose that the field would stay of uniform though reduced intensity.

In practice the source would not be an infinitely narrow slit but would have a finite though small width. This may be considered as a number of infinitely narrow slits side by side, the image of each being cut off to a slightly different extent by the knife-edge. The final intensity would be given by the sum of all these individual intensities integrated over the extent of the slit.

Thus if the geometric image of the slit is length $2s$, symmetrically disposed about the axis, and the knife-edge projects a distance x_1 over the axis, the effective knife-edge positions for the two infinitesimal elements which eventually form the upper and lower boundaries of the slit image are $(x_1 - s)$ and $(x_1 + s)$ respectively. The final intensity in the focal plane is obtained by squaring the coefficients of sin kT and cos kT in (33) and integrating their sum with respect to x_1 between these limits. If x_1 is small compared with s, so that a relatively large proportion of light passes the slit and the limits of integration are effectively $-s$ and $+s$, the illumination curve due to the upper boundary element acting alone will be very nearly that in Fig. 19, for no knife-edge, while that from the lower element will be similar to the curve for $k\theta x_1 = 0$ in the same diagram. It will be clear from the examination of the trend of these curves as the knife-edge is advanced that the intensity curve for the effect of all the elements acting together will tend towards the form of the top curve in Fig. 19, *i.e.*, will approach uniform intensity. If, on the other hand, $x_1 = s$, so that a large proportion of light is cut off, the resultant total intensity curve will lie between the curve $k\theta x_1 = 0$ and a curve of greater intensity variation even than $k\theta x_1 = \pi$. In general therefore it may be said that as the knife-edge is advanced to cut off increasing proportions of incident light to obtain greater sensitivity the uniformity of the field illumination will suffer, whether the slit is infinitely small or not.

So far no deflections in the schlieren field have been considered. It would obviously be of interest to consider instances where the general result on geometrical optical theory can be calculated and to compare this with what the more exact physical optics method gives. The case of uniform deflection over half the field, such as would be given by a prism of small angle bisecting the field of view, and the case of a small deflection over a small local area, will be taken as typical examples. The former may be considered as an increase in path R whose magnitude varies directly as θ on one side of the axis only, say $R = a\theta$ from $\theta = 0$ to $\theta = +\theta$ and $R = 0$ from $\theta = -\theta$ to $\theta = 0$. Equation (30) for the deviation of the intensity in the plane of the knife-edge thus becomes

$$\int_{-\theta}^{0} \sin k(Vt - f + x\theta)\, d\theta + \int_{0}^{\theta} \sin k(Vt - f - a\theta + x\theta)\, d\theta$$

or, if

$$Vt - f = t$$

as before,

$$\sin kT\left[\frac{\sin k\theta x}{kx} + \frac{\sin k\theta(x - a)}{k(x - a)}\right] + \cos kT\left[\frac{1 - \cos k\theta(x - a)}{k(x - a)} - \frac{1 - \cos k\theta x}{kx}\right] \ldots \quad (41)$$

THIS DOCUMENT PROVIDED BY THE ABBOTT AEROSPACE
TECHNICAL LIBRARY
ABBOTTAEROSPACE.COM

To determine what would be seen in direction ϕ, we have, as before, to replace T by $(T + \phi x)$ in (41) and integrate over the second aperture, *i.e.*, between $x = x_1$ and $x = x_2$. The coefficient of $\sin kT$ after integration becomes

$$\Big[\text{Si } k(\theta - \phi)x + \text{Si } k\phi x + \cos k\phi a \ \text{Si } k(\theta + \phi)(x - a) + \sin k\phi a \ \text{Ci } k(\theta + \phi)(x - a)$$
$$- \cos k\phi a \ \text{Si } k\phi(x - a) - \sin k\phi a \ \text{Ci } k\phi(x - a)\Big]_{x1}^{x2} \quad .. \quad .. \quad .. \quad .. \quad .. \quad (42)$$

and of $\cos kT$, is

$$\Big[\text{Ci } k(\theta - \phi)x - \text{Ci } k\phi x - \cos k\phi a \ \text{Ci } k(\theta + \phi)(x - a) + \sin k\phi a \ \text{Si } k(\theta + \phi)(x - a)$$
$$+ \cos k\phi a \ \text{Ci } k\phi(x - a) - \sin \ k\phi a \ \text{Si } k\phi(x - a)\Big]_{x1}^{x2}. \quad .. \quad .. \quad .. \quad (43)$$

Squaring (42) and (43), and adding, gives the intensity in the direction ϕ, which obviously varies with the sign of ϕ. If the knife-edge is removed, so that $x_1 = -x_2$ where x_2 is large, the intensity is found to be uniform over a large proportion of the field with a sharp fall at the edge, as shown in Fig. 20. Assuming the same dimensions of the system as were used above, Table 4 and Fig. 20 give the intensity distribution for $ka\theta = \pi$, corresponding to a uniform deviation of about $0{\cdot}4$ sec over half the field. The knife-edge positions are given by $k\theta x_1 = -\pi/4$ and $+ 0{\cdot}225\pi$. Table 5 and Fig. 21 show curves for double and half of this deviation ($ka\theta = 2\pi$ and $\pi/2$) at knife-edge positions arranged to give as uniform an intensity distribution as possible. Geometrical theory would indicate uniform illumination in the two halves of the field, the difference between the two levels being proportional to the deflection. Examination of the curves in fact shows that this is not the case, though the latter condition is roughly fulfilled.

If a slit of finite size is used instead of an infinitely narrow one, considerations similar to those applying in the case of no deflection above show that there is increasing uniformity of illumination in the two halves of the field but less difference between these as the knife-edge is withdrawn and more light passes it. This lower difference in levels would be expected on geometric optical theory but the non-uniformity when the knife-edge is advanced would not be forecast by its means. The important inference here is that, while the schlieren method may be used qualitatively to indicate the presence of extremely small deflections, great care must be used in making quantitative deductions from photographs except when the system is working at low sensitivity.

The case just discussed of a uniform deviation over half the field is useful for indicating the general capabilities of the method. It is obviously of interest however to have some idea of its sensitivity in indicating the presence of small lcal deflections. Suppose a path difference R is introduced into the beam such that

$$R = -a\alpha \text{ from } \theta = -\theta \text{ to } -\alpha$$
$$R = a\theta \quad \text{from } \theta = -\alpha \text{ to } +\alpha$$
$$R = +a\alpha \text{ from } \theta = +\alpha \text{ to } +\theta .$$

This corresponds to a small deflection at the centre of the field, symmetrical about the axis, with no deflection elsewhere. The expression (30) for the vibrations at the knife-edge becomes

$$\int_{-\theta}^{-\alpha} \sin k(T + a\alpha + x\theta)\, d\theta + \int_{-\alpha}^{+\alpha} \sin k(T - a\theta + x\theta)\, d\theta + \int_{\alpha}^{\theta} \sin k(T - a\alpha + x\theta)\, d\theta \quad .. \quad (44)$$

which reduces to

$$2 \sin kT \Big[\sin ka\alpha \frac{\cos k\theta x}{kx} - \cos ka\alpha \frac{\sin k\theta x}{kx} + \cos ka\alpha \frac{\sin k\theta x}{kx}$$
$$- \sin ka\alpha \frac{\cos k\theta x}{kx} + \frac{\sin k(x - a)\alpha}{k(x - a)}\Big]. \quad .. \quad .. \quad .. \quad (45)$$

THIS DOCUMENT PROVIDED BY THE ABBOTT AEROSPACE
TECHNICAL LIBRARY
ABBOTTAEROSPACE.COM

In order to determine the expressions for the intensity in direction ϕ, $\sin kT$ is replaced by $\sin k(T + \phi x)$ as before and the whole expression integrated between the limits x_1 and x_2. The resulting coefficient of $\sin kT$ is

$$\Big[\sin ka\alpha\ \mathrm{Ci}\ k(\alpha+\phi)x + \sin ka\alpha\ \mathrm{Ci}\ k(\alpha-\phi)x - \cos ka\alpha\ \mathrm{Si}\ k(\alpha+\phi)x$$
$$- \cos ka\alpha\ \mathrm{Si}\ k(\alpha-\phi)x + \cos ka\alpha\ \mathrm{Si}\ k(\theta+\phi)x + \cos ka\alpha\ \mathrm{Si}\ k(\theta-\phi)x$$
$$- \sin ka\alpha\ \mathrm{Ci}\ k(\theta+\phi)x - \sin ka\phi\ \mathrm{Ci}\ k(\theta-\phi)x + \sin ka\alpha\ \mathrm{Ci}\ k(\alpha+\phi)(x-a)$$
$$+ \cos ka\phi\ \mathrm{Si}\ k(\alpha+\phi)(x-a) - \sin ka\phi\ \mathrm{Ci}\ k(\alpha-\phi)(x-a)$$
$$+ \cos ka\phi\ \mathrm{Si}\ k(\alpha-\phi)(x-a\Big]_{x1}^{x2} \qquad (46)$$

and of $\cos kT$ is

$$\Big[\sin ka\alpha\ \mathrm{Si}\ k(\alpha+\phi)x - \sin ka\alpha\ \mathrm{Si}\ k(\alpha-\phi)x + \cos ka\alpha\ \mathrm{Ci}\ k(\alpha+\phi)x$$
$$- \cos ka\alpha\ \mathrm{Ci}\ k(\alpha-\phi)x - \cos ka\alpha\ \mathrm{Ci}\ k(\theta+\phi)x + \cos ka\alpha\ \mathrm{Ci}\ k(\theta-\phi)x$$
$$- \sin ka\alpha\ \mathrm{Si}\ k(\theta+\phi)x + \sin ka\alpha\ \mathrm{Si}\ k(\theta-\phi)x - \cos ka\phi\ \mathrm{Ci}\ k(\alpha+\phi)(x-a)$$
$$+ \sin ka\phi\ \mathrm{Si}\ k(\alpha+\phi)(x-a) + \cos ka\phi\ \mathrm{Ci}\ k(\alpha-\phi)(x-a)$$
$$+ \sin ka\phi\ \mathrm{Si}\ k(\alpha-\phi)(x-a)\Big]_{x1}^{x2}. \qquad (47)$$

The sum of the squares of (46) and (47) gives the intensity in the ϕ-direction and examination of the expressions shows that this will be independent of the sign of ϕ, so that the intensity distribution is symmetrical about the axis. Calculations have been made for the cases when the deflection takes place over 1/100 and 1/1000 of the total field, *i.e.*, for $\alpha/\theta = 1/100$ and $\alpha/\theta = 1/1000$; the dimensions of the system are the same as those assumed previously and knife-edge positions $k\theta x_1 = 0$ and $\pi/2$ have been taken in each case. The deflection is the same throughout, being given by $ka\theta = \pi$, corresponding to an angular deviation of $0{\cdot}4$ sec as was taken above. It was only considered necessary to calculate intensities in the region of the axis since local variations here were the main interest. Table 6 and Figs. 22 and 23 show the results. With the knife-edge on axis ($k\theta x_1 = 0$) the deflected area is only just visible as such when $\alpha/\theta = 0{\cdot}01$ and is not visible at all when $\alpha/\theta = 0{\cdot}001$, but advancing the knife-edge to $k\theta x_1 = \pi/2$ so that more light is cut off makes it visible in both cases since the eye will appreciate differences in $\log I$ of the order of $0{\cdot}02$. It is evident that further cut-off will increase the sensitivity still more. The intensity distribution over the deflecting region is again, however, unlike that forecast by geometric optics and changes in intensity could not be used to deterine the precise angle of deflection. The general conclusions therefore must be that while the schlieren system can record successfully minute deflections and so forms an excellent qualitative guide, the accuracy obtained by using it quantitatively to measure the magnitude of deflections cannot be high unless the sensitivity is low. These conclusions do not however vitiate the arguments used in the early part of this note regarding the advantages and disadvantages of different optical layouts.

6. *General Conclusions.*—The general conclusions of the investigation are that for overall ease of interpretation of results the twin-mirror system is probably the best to use, though local considerations may of course modiiy this choice, and that although the schlieren system may be used qualitatively at extremely high sensitivity its use is not recommended for quantitative work where small pressure or density changes are involved.

THIS DOCUMENT PROVIDED BY THE ABBOTT AEROSPACE
TECHNICAL LIBRARY
ABBOTTAEROSPACE.COM

REFERENCES

No.	Author	Title, etc.
1	A. Töpler	*Ann. d. Physic u. Chemie.* Vol. 131. 1867 (and other sources listed in Ref. 4).
2	Lord Rayleigh	*On the theory of small optical retardations.* Scientific Papers, Vol. VI.
3	H. Schardin	Schlieren methods and their applications. R.A.E. Translation 122.
4	N. F. Barnes and S. L. Bellinger ..	Schlieren and shadowgraph equipment for airflow analysis. *J. Opt. Soc. Amer.* August, 1945.
5	H. G. Taylor and J. M. Waldram ..	Improvements in the schlieren method. *J. Sci. Inst.* Vol. 10, p. 378. 1933.
6	E. H. Linfoot	A contribution to the theory of the Foucault test. *Proc. Roy. Soc.* Vol. 186. June, 1946.

TABLE 1

$k\theta x_1 = 0,\ k\theta x_2 = 5{,}000$

$\pm \varphi/\theta$	0	0·25	0·50	0·8	0·98	0·99	0·996	0·999	1·000	1·001	1·002	28·7
I	9·87	10·13	11·08	14·71	30·88	37·71	48·88	64·66	98·31	54·92	47·11	28·07

TABLE 2

$k\theta x_1 = \pi,\ k\theta x_2 = 5{,}000$

$\pm \varphi/\theta$	0	0·50	0·75	0·90	0·95	0·98	0·99	1·00	1·01	1·05	1·23
I	0·32	0·45	0·94	2·26	3·97	7·37	10·93	54·05	10·05	3·25	0·58

TABLE 3

$k\theta x = 5{,}000$

$\pm \varphi/\theta$	0	0·75	0·90	0·95	0·99	0·998	1·0	1·01
I	39·48	39·48	39·52	39·50	39·50	41·71	9·87	5002

TABLE 4

$ka\theta = \pi,\ k\theta x_2 = 5{,}000$

φ/θ	0	+0·01	+0·05	+0·10	+0·20	+0·50	+0·75	+0·90	+0·95	+0·99	1·00
I for $k\theta x_1 = -\pi/4$ ..	35·87	34·24	30·71	27·99	24·59	19·70	18·87	21·57	25·00	36·46	86·38
I for $k\theta x_1 = 0{\cdot}225\pi$ ..	18·85	17·66	15·21	13·39	11·24	9·10	10·20	14·10	18·38	31·42	90·91
φ/θ	0	−0·01	−0·05	−0·10	−0·20	−0·50	−0·75	−0·90	−0·95	−0·99	−1·00
I for $k\theta x_1 = -\pi/4$ ..	35·87	37·88	43·25	48·02	54·31	51·30	34·67	23·78	21·28	23·73	27·10
I for $k\theta x_1 = 0{\cdot}225\pi$ ..	18·85	20·05	23·96	27·44	32·64	39·43	37·30	34·27	34·22	39·76	72·72

THIS DOCUMENT PROVIDED BY THE ABBOTT AEROSPACE
TECHNICAL LIBRARY
ABBOTTAEROSPACE.COM

TABLE 5

$k\theta x_2 = 5{,}000$

φ/θ	0	+0·004	+0·010	+0·02	+0·05	+0·10	+0·20	+0·50	0·75
I for $ka\theta = 2\pi$, $k\theta x_1 = 3\pi/2$	11·56	9·14	10·09	9·16	7·30	5·51	3·65	1·762	1·415
I for $ka\theta = \pi/2$, $k\theta x_1 = 0$	—	19·97	20·02	19·56	18·54	17·39	15·96	14·57	15·96
φ/θ	0·90	0·95	1·00	−0·004	- 0·010	−0·02	−0·05	−0·10	−0·20
I for $ka\theta = 2\pi$ $k\theta x_1 = 3\pi/2$	1·85	2·72	37·34	10·54	12·50	13·03	14·09	15·19	16·67
I for $ka\theta = \pi/2$ $k\theta x_1 = 0$	20·12	—	—	21·23	21·39	21·92	23·20	24·79	27·06
φ/θ	+0·50	−0·75	−0·90	−0·95	−1·000				
I for $ka\theta = 2\pi$, $k\theta x_1 = 3\pi/2$	19·25	21·02	23·80	26·92	84·77				
I for $ka\theta = \pi/2$, $k\theta x_1 = 0$	30·16	30·49	31·59	33·73					

TABLE 6

$ka\theta = \pi$, $k\theta x_2 = 5{,}000$

		$\pm\varphi/\theta$	0	0·001	0·002	0·005	0·01	0·02	0·05	0·10	0·20
I	$k\theta x_1 = 0$	$\alpha/\theta = 0{\cdot}01$	12·20	—	—	12·15	11·90	11·50	11·12	10·88	—
		$\alpha/\theta = 0{\cdot}001$	10·18	10·15	10·12	—	10·10	—	10·00	—	—
	$k\theta x_1 = \pi/2$	$\alpha/\theta = 0{\cdot}01$	0·516	—	—	—	0·464	0·386	0·319	—	—
		$\alpha/\theta = 0{\cdot}001$	0·199	0·195	0·192	—	0·182	—	0·169	—	0·195
		$\pm\varphi/\theta$	0·30	0·50							
I	$k\theta x_1 = \theta$	$\alpha/\theta = 0{\cdot}01$	10·83	11·51							
		$\alpha/\theta = 0{\cdot}001$	10·31	—							
	$k\theta x_1 = \pi/2$	$\alpha/\theta = 0{\cdot}01$	0·293	—							
		$\alpha/\theta = 0{\cdot}001$	—	—							

THIS DOCUMENT PROVIDED BY THE ABBOTT AEROSPACE
TECHNICAL LIBRARY
ABBOTTAEROSPACE.COM

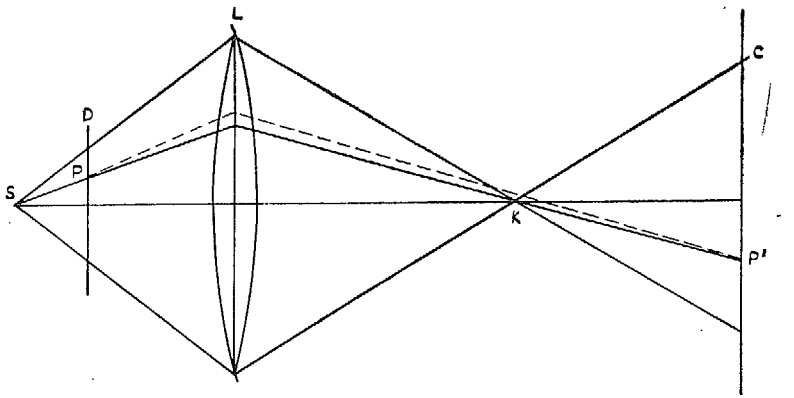

FIG. 1. The simple schlieren system.

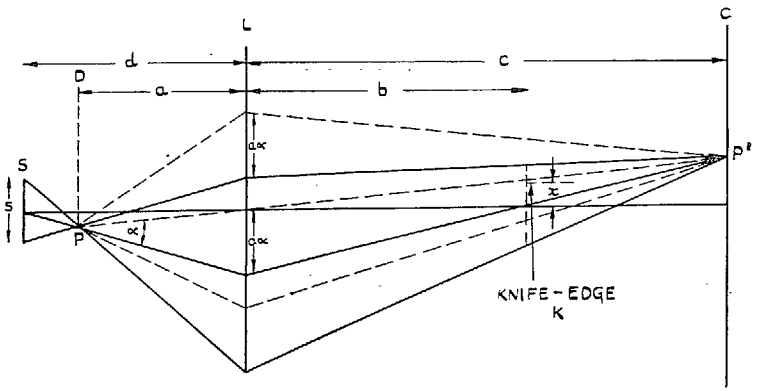

FIG. 2. Schlieren system with finite slit.

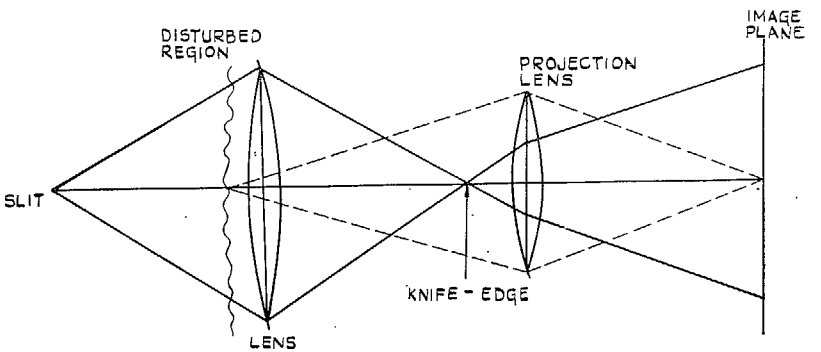

FIG. 3. The use of a subsidiary lens for projection.

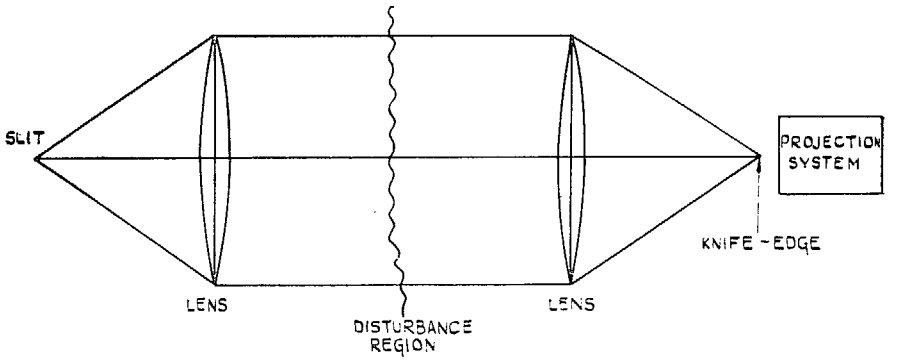

FIG. 4. The two-lens parallel-beam system.

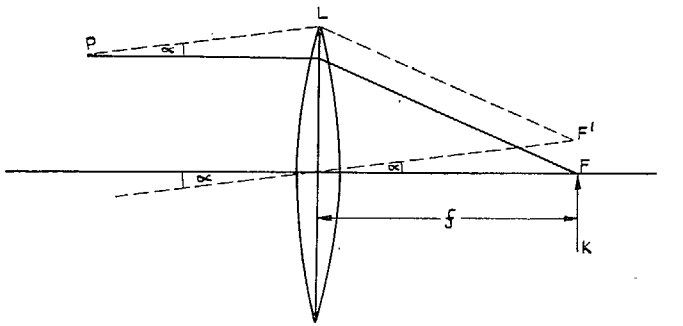

FIG. 5. Displacement caused at the knife-edge.

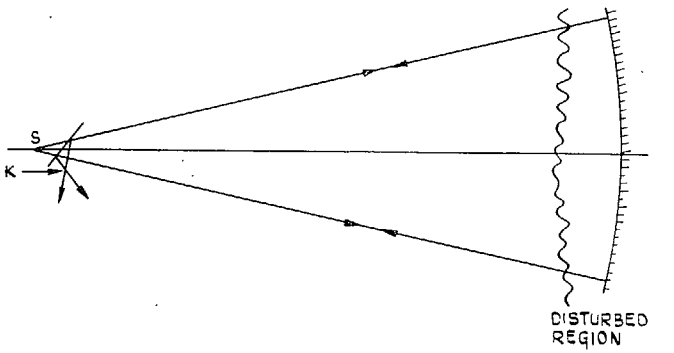

FIG. 6. Single-mirror system.

THIS DOCUMENT PROVIDED BY THE ABBOTT AEROSPACE
TECHNICAL LIBRARY
ABBOTTAEROSPACE.COM

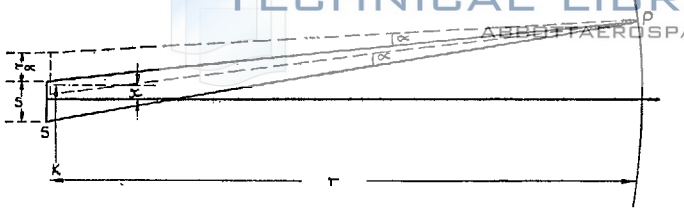

FIG. 7. Effect of errors on mirror surface.

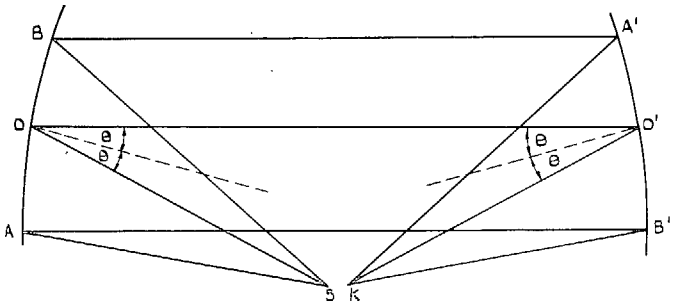

FIG. 10. Unsymmetrical twin-mirror system.

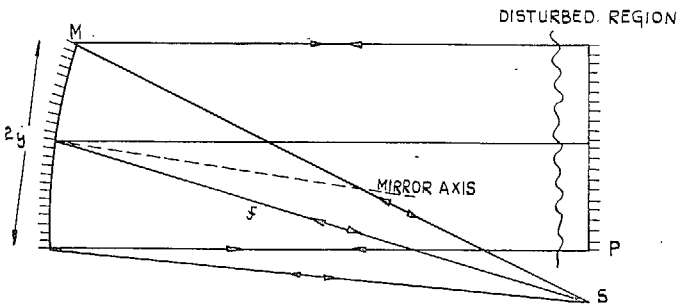

FIG. 8. Plane-concave mirror system.

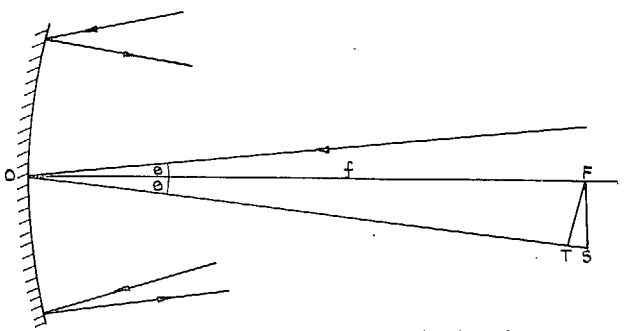

FIG. 11. Astigmatic foci for a single mirror.

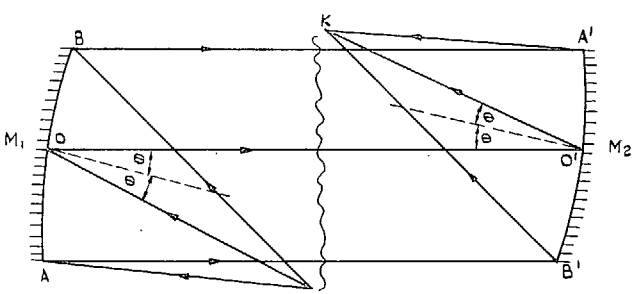

FIG. 9. Twin-mirror system.

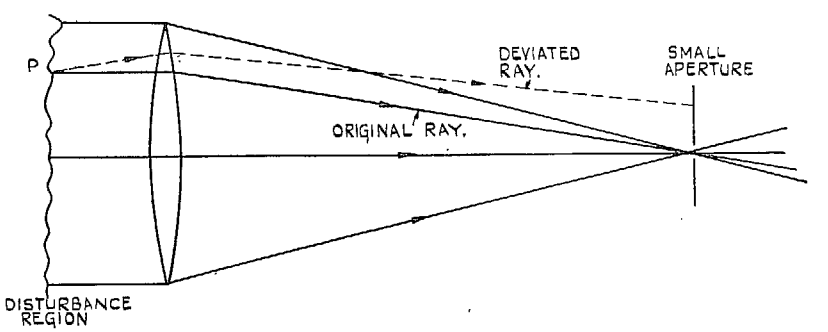

FIG. 12. Principal of Santon's method.

THIS DOCUMENT PROVIDED BY THE ABBOTT AEROSPACE
TECHNICAL LIBRARY
ABBOTTAEROSPACE.COM

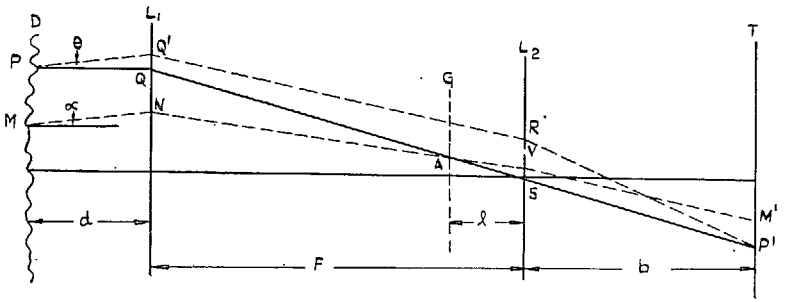

FIG. 13. Principal of Ronchi method.

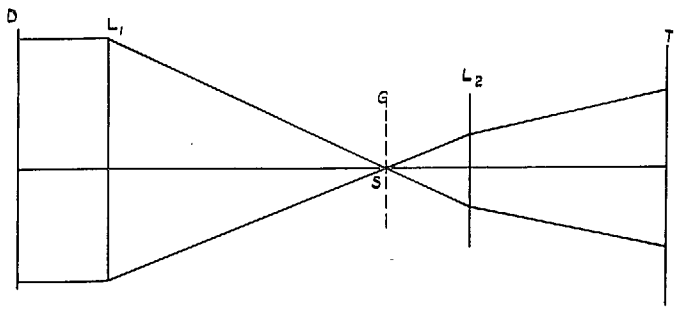

FIG. 14. Ronchi ' isophot ' method.

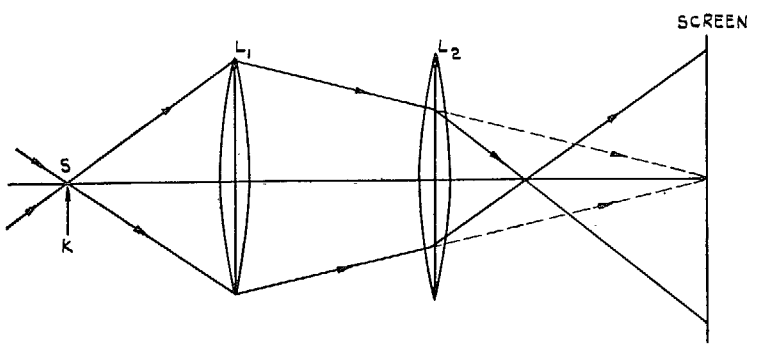

FIG. 15. Two-lens projection system.

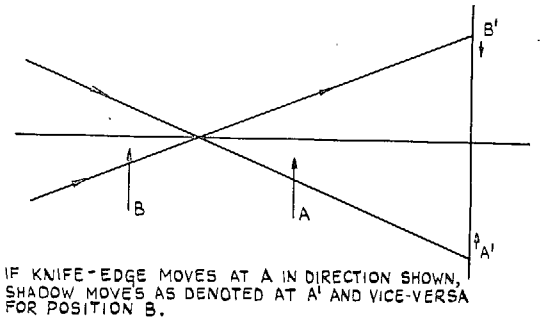

FIG. 16. Movement of shadow as knife-edge changes.

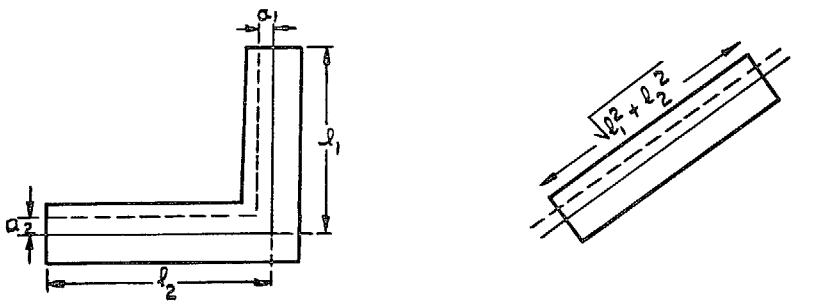

FIG. 17. Comparison of L-shaped and straight knife-edges.

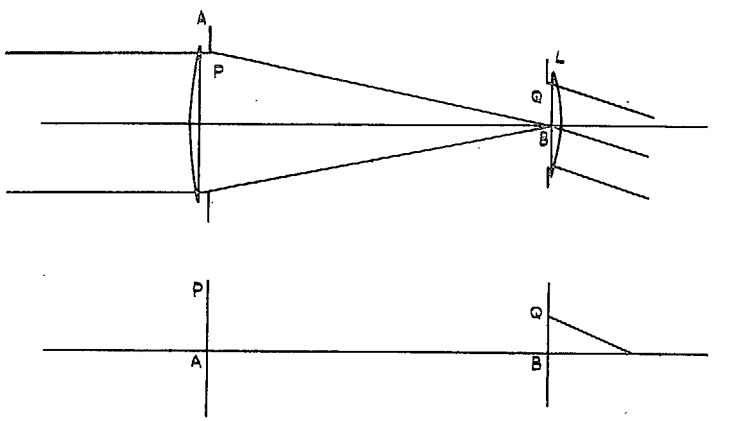

FIG. 18. The fundamental schlieren theory.

THIS DOCUMENT PROVIDED BY THE ABBOTT AEROSPACE
TECHNICAL LIBRARY
NO KNIFE-EDGE ABBOTTAEROSPACE.COM

(61797) Wt. 17/680 K.9 11/54 Hw.

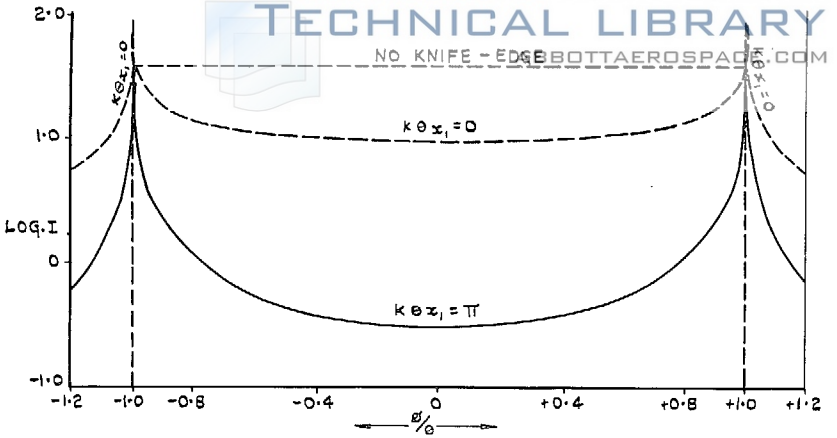

FIG. 19. Intensity distribution with no deflection.

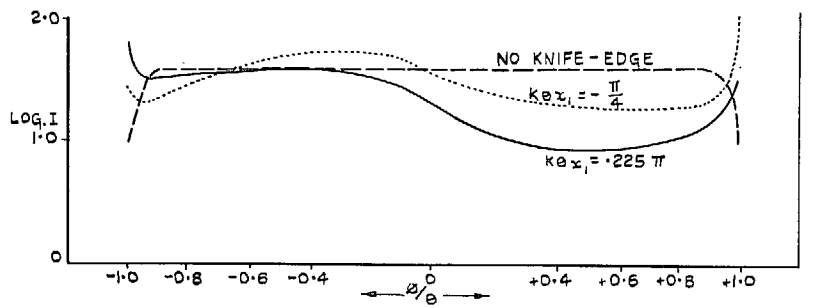

FIG. 20. Intensity distribution with deflection $ka\theta = \pi$.

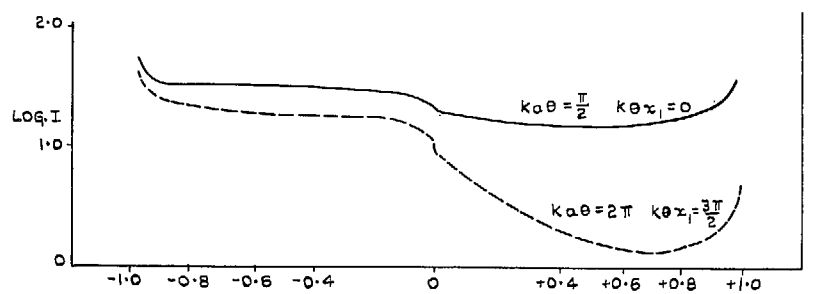

FIG. 21. Intensity distribution for deflections $ka\theta = \pi/2$ and 2π.

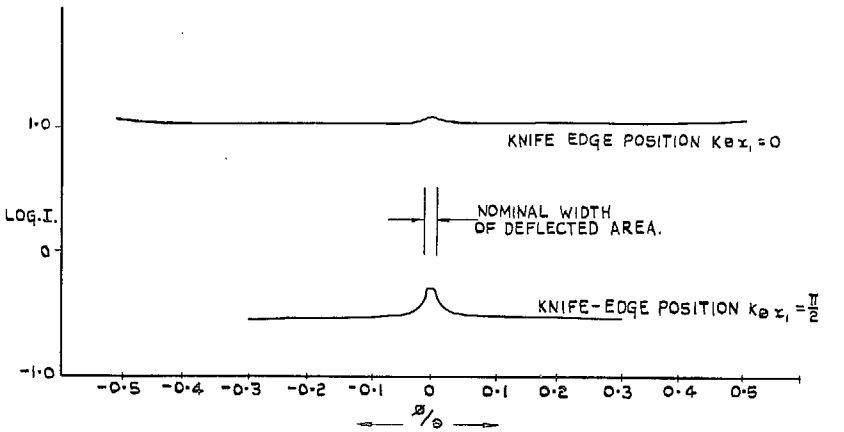

FIG. 22. Intensity distribution for $\alpha/\theta = 0{\cdot}01$, $ka\theta = \pi$.

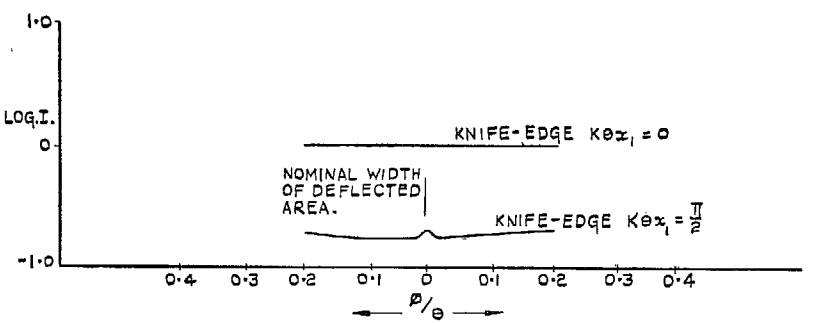

FIG. 23. Intensity distribution for $\alpha/\theta = 0{\cdot}001$, $ka\theta = \pi$.

PRINTED IN GREAT BRITAIN

THIS DOCUMENT PROVIDED BY THE ABBOTT AEROSPACE
TECHNICAL LIBRARY
ABBOTTAEROSPACE.COM

Publications of the Aeronautical Research Council

ANNUAL TECHNICAL REPORTS OF THE AERONAUTICAL RESEARCH COUNCIL (BOUND VOLUMES)

1936 Vol. I. Aerodynamics General, Performance, Airscrews, Flutter and Spinning. 40*s.* (41*s.* 1*d.*)
Vol. II. Stability and Control, Structures, Seaplanes, Engines, etc. 50*s.* (51*s.* 1*d.*)

1937 Vol. I. Aerodynamics General, Performance, Airscrews, Flutter and Spinning. 40*s.* (41*s.* 1*d.*)
Vol. II. Stability and Control, Structures, Seaplanes, Engines, etc. 60*s.* (61*s.* 1*d.*)

1938 Vol. I. Aerodynamics General, Performance, Airscrews. 50*s.* (51*s.* 1*d.*)
Vol. II. Stability and Control, Flutter, Structures, Seaplanes, Wind Tunnels, Materials. 30*s.* (31*s.* 1*d.*)

1939 Vol. I. Aerodynamics General, Performance, Airscrews, Engines. 50*s.* (51*s.* 1*d.*)
Vol. II. Stability and Control, Flutter and Vibration, Instruments, Structures, Seaplanes, etc. 63*s.* (64*s.* 2*d.*)

1940 Aero and Hydrodynamics, Aerofoils, Airscrews, Engines, Flutter, Icing, Stability and Control, Structures, and a miscellaneous section. 50*s.* (51*s.* 1*d.*)

1941 Aero and Hydrodynamics, Aerofoils, Airscrews, Engines, Flutter, Stability and Control, Structures. 63*s.* (64*s.* 2*d.*)

1942 Vol. I. Aero and Hydrodynamics, Aerofoils, Airscrews, Engines. 75*s.* (76*s.* 3*d.*)
Vol. II. Noise, Parachutes, Stability and Control, Structures, Vibration, Wind Tunnels. 47*s.* 6*d.* (48*s.* 7*d.*)

1943 Vol. I. Aerodynamics, Aerofoils, Airscrews. 80*s.* (81*s.* 4*d.*)
Vol. II. Engines, Flutter, Materials, Parachutes, Performance, Stability and Control, Structures. 90*s.* (91*s.* 6*d.*)

1944 Vol. I. Aero and Hydrodynamics, Aerofoils, Aircraft, Airscrews, Controls. 84*s.* (85*s.* 8*d.*)
Vol. II. Flutter and Vibration, Materials, Miscellaneous, Navigation, Parachutes, Performance, Plates and Panels, Stability, Structures, Test Equipment, Wind Tunnels. 84*s.* (85*s.* 8*d.*)

Annual Reports of the Aeronautical Research Council—

1933–34	1*s.* 6*d.* (1*s.* 8*d.*)	1937	2*s.* (2*s.* 2*d.*)
1934–35	1*s.* 6*d.* (1*s.* 8*d.*)	1938	1*s.* 6*d.* (1*s.* 8*d.*)
April 1, 1935 to Dec. 31, 1936	4*s.* (4*s.* 4*d.*)	1939–48	3*s.* (3*s.* 2*d.*)

Index to all Reports and Memoranda published in the Annual Technical Reports, and separately—

April, 1950 - - - - R. & M. No. 2600. 2*s.* 6*d.* (2*s.* 7½*d.*)

Author Index to all Reports and Memoranda of the Aeronautical Research Council—

1909–1949. R. & M. No. 2570. 15*s.* (15*s.* 3*d.*)

Indexes to the Technical Reports of the Aeronautical Research Council—

December 1, 1936 — June 30, 1939.	R. & M. No. 1850.	1*s.* 3*d.* (1*s.* 4½*d.*)
July 1, 1939 — June 30, 1945.	R. & M. No. 1950.	1*s.* (1*s.* 1½*d.*)
July 1, 1945 — June 30, 1946.	R. & M. No. 2050.	1*s.* (1*s.* 1½*d.*)
July 1, 1946 — December 31, 1946.	R. & M. No. 2150.	1*s.* 3*d.* (1*s.* 4½*d.*)
January 1, 1947 — June 30, 1947.	R. & M. No. 2250.	1*s.* 3*d.* (1*s.* 4½*d.*)
July, 1951.	R. & M. No. 2350.	1*s.* 9*d.* (1*s.* 10½*d.*)

Prices in brackets include postage.

Obtainable from

HER MAJESTY'S STATIONERY OFFICE

York House, Kingsway, London, W.C.2; 423 Oxford Street, London, W.1 (Post Orders: P.O. Box 569, London, S.E.1); 13a Castle Street, Edinburgh 2; 39, King Street, Manchester 2; 2 Edmund Street, Birmingham 3; 1 St. Andrew's Crescent, Cardiff; Tower Lane, Bristol 1; 80 Chichester Street, Belfast, or through any bookseller

S.O. Code No. 23-2859